Pergamon

Int. J. Heat Mass Transfer. Vol. 39, No. 4, pp. 867–875, 1996

0017–9310/96 $15.00 + 0.00

0017–9310(95)00069–0

Numerical study of steady laminar fully developed fluid flow and heat transfer in rectangular and elliptical ducts rotating about a parallel axis

M. MAHADEVAPPA,† V. RAMMOHAN RAO and V. M. K. SASTRI‡

Department of Mechanical Engineering, Indian Institute of Technology, Madras 600 036, India

(*Received* 31 *October* 1992 *and in final form* 29 *November* 1994)

Abstract—A numerical study, using the finite-difference method (FDM) has been carried out to obtain fluid flow and heat transfer characteristics in respect of rectangular and elliptical ducts, rotating about a parallel axis situated parallel to and away from their axes. The study encompasses many geometries for the rotating as well as stationary duct sections under laminar developed flow conditions for various Prandtl numbers and aspect ratios. The investigation is made for the parameters Nu/Nu_0, $Ra\ Re$, $(fRe)/(fRe)_0$ and Pr. Correlations for heat transfer in the cases of rotating rectangular and elliptical ducts have been presented. From the study, it has been concluded that elliptical geometry is superior to others that are frequently used as coolant channels in rotating machinery.

1. INTRODUCTION

The overall trend in the design of turbo-alternators and induction motors all over the world, has been towards increased power output while retaining or even reducing the size of the machine. One of the crucial factors affecting such a design procedure is the design of the coolant channels provided inside the conductors. While there are many considerations deciding the overall size of these coolant channels, there is the vital aspect of the associated fluid flow and heat transfer which has a direct bearing on the ultimate rating of the machine in as much as this aspect affects the reliability of the electrical insulation provided for. The complexity of the phenomena of fluid flow and heat transfer occurring in these coolant channels is further compounded by the rotating nature of these channels, their configuration and relative orientation. Under these circumstances any improved understanding of these phenomena helps in optimizing the design procedures involved.

Until recently, designers have generally ignored the effect of rotation in the thermal design of motors. However, it has been established that rotation considerably enhances the heat transfer in a coolant channel due to the influence of the secondary flows arising out of rotation. But quantitative information in this area of interest has been very much limited and in some specific cases no information is available to-date. Studies in this field are reported in the literature, but the majority of them are directed towards investigations concerning the simplest of the geometries, the circular ducts.

Fluid flow and heat transfer in respect of various geometries (including elliptical sections) have been discussed by Shah and London [1] and Kakac *et al.* [2] for stationary ducts. Analytical studies about rotating ducts of circular, square and rectangular geometries have been presented by Morris [3].

Numerical studies of rotating circular ducts have been published by Woods and Morris [4], and Majumdar *et al.* [5]. Numerical investigation of rotating rectangular ducts has been reported by Morris and Dias [6], Sarunac *et al.* [7] and Neti *et al.* [8]. It has been observed from the literature survey that rotating rectangular ducts have not been studied systematically to cover any wider range of parameters such as aspect ratio, eccentricity ratio and Prandtl number. Also it has been found that no work, analytical, numerical or experimental, has been reported to-date on the enhancement aspect of heat transfer and fluid flow in rotating elliptical ducts, though this geometry constitutes a useful family of ducts, ranging from narrow lenticular passages to circular passages.

This paper presents a numerical study, using a finite-difference method for fluid flow and heat transfer characteristics of rotating rectangular and elliptical ducts for a wide range of parameters, namely aspect

† Present address: Assistant Professor, Department of Mechanical Engineering, S. J. College of Engineering, Mysore, India.

‡ Author to whom correspondence should be addressed.

NOMENCLATURE

a	semi major axis of an elliptical duct [m]
a_φ	coefficient in the modified general elliptical equation
AR	aspect ratio, a/b
b	semi minor axis of an elliptical duct [m]
D_H	hydraulic diameter [m]
D_φ	the source term in the general elliptic equation
f	dimensionless pressure drop $[(dp/dz)D_H]/(1/2\rho_b w_m^2)$
f_0	friction factor for stationary duct
H'	distance between the axis of rotation and the longitudinal axis of the duct [m]
H	H'/D_H
h	convective heat transfer coefficient [W m^{-2} K^{-1}]
J	rotational Reynolds number, $\Omega D_H^2/\nu$
k	thermal conductivity of the fluid [W m^{-1} K^{-1}]
Nu_0	Nusselt number for stationary tube
Nu	Nusselt number, hD_H/k
p	pressure [Pa]
Pr	Prandtl number
Re	through flow Reynolds number, $w_m D_H/\nu$
T	temperature [K]
w_m	mean axial velocity [m s^{-1}]
u, v, w	velocity components [m s^{-1}]
U, V, W	dimensionless velocity components
x, y, z	Cartesian coordinates
X, Y, Z	dimensionless Cartesian coordinates.

Greek symbols

α	thermal diffusivity of fluid [m^2 s^{-1}]
β	coefficient of thermal expansion of fluid [K^{-1}]
ε	eccentricity parameter, H'/D_H
Θ	non-dimensional temperature
μ	viscosity [N s m^{-2}]
ξ	vorticity
ρ	density [kg m^{-3}]
ν	kinematic viscosity of fluid [m^2 s^{-1}]
τ	axial temperature gradient, $\partial T/\partial z = \partial T_b/\partial z$ [K m^{-1}]
ψ	stream function
Ω	angular velocity.

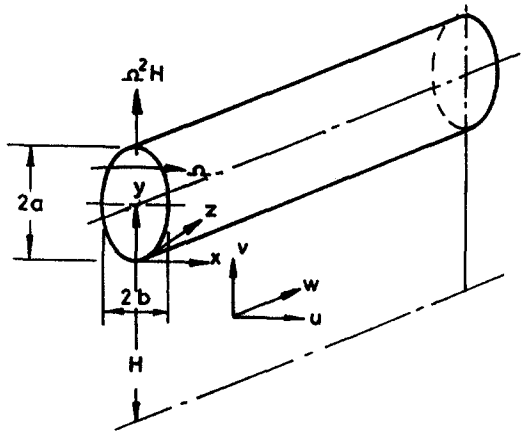

Fig. 1. Physical model and co-orinate system for rotating elliptic tube.

ratio, eccentricity ratio, ($Ra\ Re$), and Prandtl number for fully developed laminar flow.

2. GOVERNING EQUATIONS AND SOLUTION PROCEDURE

The governing equations for the fluid flow and heat transfer, for the physical model shown in Fig. 1, are given below. The assumptions made are:

1. the fluid is Newtonian
2. flow is laminar and fully developed
3. the Boussinesq approximation is valid
4. the duct is supplied with constant heat flux axially and the circumferential temperature is uniform, i.e. H1 boundary condition
5. no internal heat generation.

Continuity equation:

$$\frac{\partial u}{\partial x}+\frac{\partial v}{\partial y}=0. \tag{1}$$

X-momentum equation:

$$u\frac{\partial u}{\partial x}+v\frac{\partial u}{\partial y}=-\frac{1}{\rho}\frac{\partial p}{\partial x}-2\Omega\beta(T_w-T)v$$
$$+\Omega^2\beta(T_w-T)x+\nu\left(\frac{\partial^2 u}{\partial x^2}+\frac{\partial^2 u}{\partial y^2}\right). \tag{2}$$

Y-momentum equation:

$$u\frac{\partial v}{\partial x}+v\frac{\partial v}{\partial y}=-\frac{1}{\rho}\frac{\partial p}{\partial y}+2\Omega\beta(T_w-T)u$$
$$+\Omega^2\beta(T_w-T)(H'+y)+\nu\left(\frac{\partial^2 v}{\partial x^2}+\frac{\partial^2 v}{\partial y^2}\right). \tag{3}$$

Z-momentum equation:

$$u\frac{\partial w}{\partial x}+v\frac{\partial w}{\partial y}=-\frac{1}{\rho}\frac{dp}{dz}+\nu\left(\frac{\partial^2 w}{\partial x^2}+\frac{\partial^2 w}{\partial y^2}\right). \tag{4}$$

Energy equation:

$$u\frac{\partial T}{\partial x}+v\frac{\partial T}{\partial y}=-w\frac{\mathrm{d}T}{\mathrm{d}z}+\alpha\left(\frac{\partial^2 T}{\partial x^2}+\frac{\partial^2 T}{\partial y^2}\right). \quad (5)$$

Stream function and vorticity are introduced to eliminate the pressure terms from the x and y momentum equations. Stream function: $u=(\partial\psi'/\partial y)$ and $v=-(\partial\psi'/\partial x)$,

vorticity:

$$\xi'=\frac{\partial v}{\partial x}-\frac{\partial u}{\partial y}\Rightarrow\xi'=-\nabla^2\psi'$$

then

$$\frac{\partial(3)}{\partial x}-\frac{\partial(2)}{\partial y}\Rightarrow u\frac{\partial\xi'}{\partial x}+v\frac{\partial\xi'}{\partial y}=-2\Omega\beta\left(u\frac{\partial T}{\partial x}+v\frac{\partial T}{\partial y}\right)$$
$$-\Omega^2\beta\left(x\frac{\partial T}{\partial y}-(H'+y)\frac{\partial T}{\partial x}\right)+\nu\nabla^2\xi'.$$

Non-dimensionalization is carried out as follows:

$$U=\frac{uD_H}{\nu}\quad V=\frac{vD_H}{\nu}\quad W=\frac{wD_H}{\nu}$$

$$\Theta=\frac{(T_w-T)}{\tau D_H Pr}\quad \xi=\frac{\xi' D_H^2}{\nu}\quad \psi=\frac{\psi'}{\nu}$$

$$x=\frac{x}{D_H}\quad Y=\frac{y}{D_H}\quad H=\frac{H'}{D_H}$$

where $Pr=\nu/\alpha$ and $\tau=\mathrm{d}T/\mathrm{d}z=\partial T/\partial z$ (specified axial temperature gradient, as a consequence of H1 type boundary condition).

The final form of equations (1)–(5) after introducing the stream function and vorticity and non-dimensionalization is as follows:

$$\frac{\partial^2\psi}{\partial X^2}+\frac{\partial^2\psi}{\partial Y^2}+\xi=0 \quad (6)$$

$$\frac{\partial(\psi,\xi)}{\partial(X,Y)}+\left(\frac{\partial^2\xi}{\partial X^2}+\frac{\partial^2\xi}{\partial Y^2}\right)-\frac{2Ra}{J}\frac{\partial(\psi,\theta)}{\partial(X,Y)}$$
$$-Ra\left(X\frac{\partial\theta}{\partial Y}-(H+Y)\frac{\partial\theta}{\partial X}\right)=0 \quad (7)$$

$$\frac{\partial(\psi,W)}{\partial(X,Y)}+\left(\frac{\partial^2 W}{\partial X^2}+\frac{\partial^2 W}{\partial Y^2}\right)+Re_p=0 \quad (8)$$

$$Pr\left[\frac{\partial(\psi,\theta)}{\partial(X,Y)}\right]+\left(\frac{\partial^2\theta}{\partial X^2}+\frac{\partial^2\theta}{\partial Y^2}\right)+W=0 \quad (9)$$

where $\partial(\psi,\xi)/\partial(X,Y)$ is the Jacobian defined as

$$\frac{\partial\psi}{\partial X}\frac{\partial\xi}{\partial Y}-\frac{\partial\psi}{\partial Y}\frac{\partial\xi}{\partial X}$$

$$Ra=\frac{\Omega^2\beta\tau D_H^5}{\alpha\nu}\quad J=\frac{\Omega D_H^2}{\nu}\quad\text{and}\quad Re_p=-\frac{D_H^3}{\rho\nu^2}\frac{\partial p}{\partial z}.$$

A control volume integrated finite-differences method similar to the method used by Gosman *et al.* [9] has been used to solve the above set of differential equations. Table 1 gives comparison of the above equations (6)–(9) with the general conservation equation the solution procedure for which has been derived by Gosman *et al.* [9].

Table 1.

ϕ	a_ϕ	D_ϕ
ψ	0	$-\xi$
ξ	1	$\frac{2Ra}{J}\frac{\partial(\psi,\theta)}{\partial(X,Y)}-Ra\left(X\frac{\partial\theta}{\partial Y}-(H+Y)\frac{\partial\theta}{\partial X}\right)$
W	1	$-Re_p$
η	Pr	$-W$

$$\underbrace{a_\phi\left[\frac{\partial\psi}{\partial X}\frac{\partial\phi}{\partial Y}-\frac{\partial\psi}{\partial Y}\frac{\partial\phi}{\partial X}\right]}_{\text{convection}}-\underbrace{\left[\frac{\partial^2\phi}{\partial X^2}+\frac{\partial^2\phi}{\partial Y^2}\right]}_{\text{diffusion}}+\underbrace{D_\phi}_{\text{source}}=0 \quad (10)$$

3. GRID SYSTEM

The rectangular domain (Fig. 2) is discretized using the parametric equations of an ellipse, i.e. $X=b\cos\theta$ and $Y=a\sin\theta$, where a and b are respectively the semi-major and semi-minor axes of the ellipse. To get an elliptical domain, a certain portion of the rectangle is blocked as shown in Fig. 2. Thus an approximate ellipse is constructed from the discretized rectangular domain. This type of discretization has an inherent advantage besides extracting a proper ellipse from a rectangle. The grid will be finer near the boundaries (at least normal to the boundary) where velocity/temperature gradients are expected to be large. The blockage ignores roughly half of the total number of nodes. For example, a 21×21 grid would consist of a total of 441 nodes if the domain were rectangular. If the elliptical portion only is considered, the number of nodes becomes 221. Thus one would essentially work with a 15×15 grid.

4. BOUNDARY CONDITIONS

4.1. *Rectangular duct*

a. *Stream function.* As the duct walls are impermeable, on the four boundaries, the stream function has a constant value; for example, a value of 1 was assigned.

b. *Axial velocity.* Axial velocity was assigned as zero on the boundaries (no-slip condition).

c. *Temperature.* From the non-dimensionalization it can be seen that the non-dimensional temperature θ is 0 on the walls.

d. *Vorticity.* The boundary conditions for vorticity are not straightforward and have to be obtained from

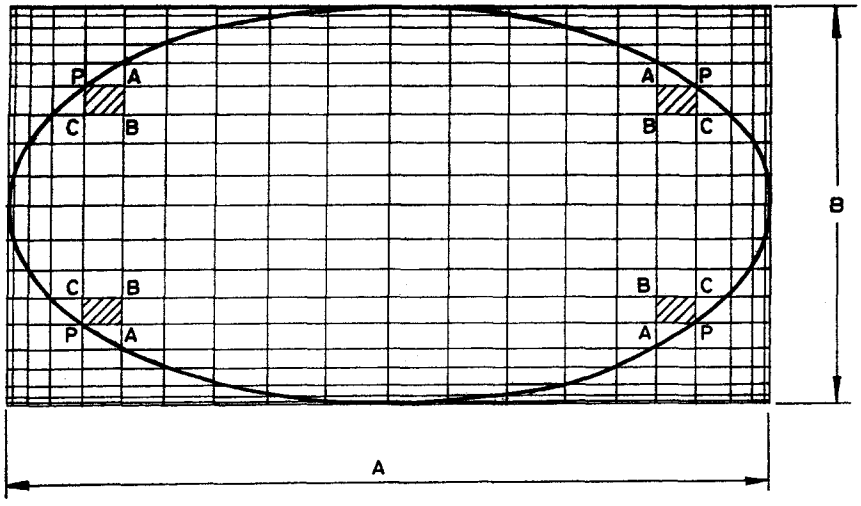

Fig. 2. Grid system. Aspect ratio = B/A.

the known information in the neighborhood of the node on the boundary [9].

A cubic polynomial is fitted for the stream function near the boundary in terms of the coordinate normal to the boundary (refer to Fig. 3). i.e. $\psi = a\ s^3 + b\ s^2 + cs + d$

The conditions available to evaluate the constants, a, b, c and d are

1. ψ is known at node (1) and (2)
2. ξ is known at node (2)
3. $\partial\psi/\partial s$ is zero on the wall at node (1) (no-slip condition).

Using these conditions and the definition of vorticity ξ (equation (6)) the expression for vorticity on the boundary is obtained.

In general, if w refers to the node on the wall and n refers to neighboring node then

$$\xi_w = -(3(\psi_n - \psi_w)/r^2) - (\xi_n/2)$$

where r is the distance between the wall and the neighboring node (further details are available in Gosman *et al.* [9]).

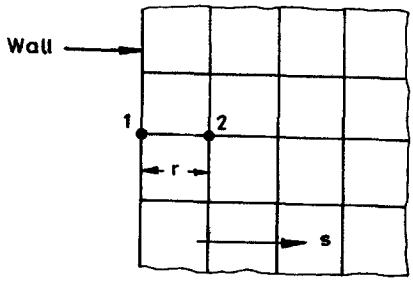

Fig. 3. Notation for boundary condition of a rectangular geometry.

4.2. *Elliptic duct*

For the elliptic duct, the first three boundary conditions, namely for stream function, axial velocity and temperature, are the same as those for a rectangular duct as mentioned earlier.

For the vorticity boundary condition the assumption made in the earlier case will not be valid as is seen from Fig. 4. In this case, ψ will depend on both X and Y coordinates as none of the coordinate axes may be normal to the boundary. One can try to interpolate ξ at the wall from the conditions known at the three neighboring nodes. These nodes have to be selected such that the normal drawn at the point passes through the area of the element as shown in Fig. 2. The known conditions are (refer to Fig. 4):

1. ψ are known at four nodes (4)
2. ξ are known at three neighboring nodes (3)
3. $\partial\psi/\partial x$, $\partial\psi/\partial y$ are zero at the wall node (velocities vanish on the wall, no-slip condition, (2)).

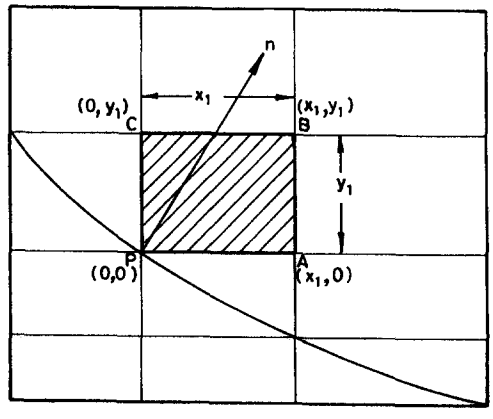

Fig. 4. Notation for boundary conditions of an elliptical geometry.

Thus a total of 9 conditions are available. So one can use a cubic polynomial in X, Y as follows:

$$\psi = a(x^3+y^3)+bx^2y+cxy^2+dx^2 + ey^2+fxy+gx+hy+k$$

which involves nine constants to be evaluated. These constants are to be evaluated using the available conditions given above. Then the value of stream function on the boundary node can be calculated using

$$\xi_1 = -\left(\frac{\partial^2\psi}{\partial X^2}+\frac{\partial^2\psi}{\partial Y^2}\right)\Bigg|_{\substack{x=0\\y=0}}$$

From the above it can be seen that the number of constants to be found is reduced from 9 to 6 due to direct availability of three constants namely g, h and k. A closed form solution for the above set of equations is very tedious to obtain unlike in the earlier case of a rectangular duct. However, in the present study, for each node on the boundary, the equations are solved by the Gauss elimination technique. It is very important to note that the neighboring nodes for the node on the boundary should be chosen such that the normal to the boundary passes through the rectangular area. This can be seen from Fig. 4.

5. RESULTS AND DISCUSSION

5.1. *Analysis*

In the present study, the effect of Rayleigh number (Ra), Reynolds number (Re), eccentricity (ε), and rotational Reynolds number (J) on heat transfer (Nu) and flow resistance (fRe) are examined. The theoretical model seemingly requires Ra, Re, Pr, J and ε to be independently specified. However, it has been shown in [3] that the product $Ra\,Re$ is a naturally emerging group, so the independent specification of Ra and Re is unnecessary. This was actually shown by Woods and Morris [4] using the following transformation,

$$\bar{\psi} = Pr\psi \quad \bar{\xi} = Pr\xi \quad \bar{W} = W/Re_p \quad \text{and} \quad \bar{\eta} = \eta/Re_p.$$

This was confirmed by experiments and numerical studies by other researchers e.g. Neti *et al.* [8] Levy *et al.* [11] and is a well established result. In fact this was confirmed by running the program with different Ra–Re combinations to get the same $Ra\,Re$ product. This reduces the amount of computational labor needed to examine the effect of various parameters influencing the problem. In Table 1, Ra, J, Re_p and H are based on the reference length parameter L, but for interpretation of data, these have to be based on the hydraulic diameter D_H. Once the geometry was fixed (i.e. aspect ratio is fixed), the relationship between L and D_H was obtained prior to the solution of the equations in the Table 1. This relationship was made use of to prescribe the desired values for the parameters Ra, J, Re_p and H based on the hydraulic diameter. The range of parameters covered in the present investigation is given in Table 2. This covers a wide range of parameters that occur in practice [3].

Table 2. Range of parameters considered in the present numerical study

$Ra\,Re$	10^3	10^4	10^5	10^6		
Pr	0.7	1.0	2.0	4.0	6.0	
AR	0.1	0.2	0.4	0.6	0.8	1.0
	1.25	1.67	2.5	5.0	10.0	
J	5.0	10.0	20.0	50.0	100.0	
ε	1.0	2.0	3.0	4.0	5.0	50

The through-flow Reynolds number Re (which is based on the mean axial velocity w_m) can be calculated only after obtaining the solution for the governing equations. The relationship between the pseudo Reynolds number Re_p and Re was found to be nonlinear and not known *a priori*. Hence it looks as if it is not possible to specify the product $Ra\,Re$ for the problem. However, with a small effort this was made possible. The methodology is described in the following paragraph.

As independent specification of Ra and Re is not required, the input value for Ra was fixed at 100 for all the calculations. A guess value for Re_p was prescribed initially and this value was suitably adjusted for every 50 iterations to get a desired value of the product $Ra\,Re$. This procedure worked very well and by the time a converged solution was obtained, $Ra\,Re$ approached the desired value within $\pm 1\%$. This is not a wasteful effort as the results were obtained for a desired set of $Ra\,Re$ values. The additional computational time to do this was practically negligible as the solution procedure itself was of an iterative nature.

5.2. *Results for stationary ducts*

The solution method is verified with different grid sizes for stationary rectangular and elliptic ducts. For grid sizes 15×15, 21×21 and 31×31, the results showed maximum errors of 3%, 1.5%, and 1.2% respectively compared with the exact analytical values available in the literature. As the higher order grid sizes need more computational time, as a good compromise, a 21×21 grid size is used in the present computation. Tables 3 and 4 compare the present Nusselt number and fRe for various aspect ratios with those of Shah and London [1].

5.3. *Results for rotating ducts*

For an aspect ratio of 0.4, Fig. 5 gives the variation of Nu/Nu_0 (the ratio of Nusselt number for the rotating duct to that for the stationary duct) with $Ra\,Re$ at different Prandtl numbers for an elliptical duct, whereas Fig. 6 shows the variation of the ratio Nu/Nu_0 with $Ra\,Re$ in the case of rectangular duct for different Prandtl numbers. For any particular Pr, the ratio Nu/Nu_0 gradually increases with $Ra\,Re$ at an almost constant slope. The Nusselt number ratio becomes greater than 1 as $Ra\,Re$ increases. The figure shows

Table 3. Comparison of Nusselt number and friction factor data for a stationary elliptical duct for various aspect ratios

	Nu		*f*Re*		% error	
AR	Exact	Present	Exact	Present	*Nu*	*f*Re*
0.2	4.962	4.8871	18.602	18.9142	1.509	−1.678
0.4	4.666	4.5943	17.294	17.5840	1.537	−1.677
0.5	4.558	4.4874	16.823	17.1056	1.549	−1.680
0.6	4.477	4.4074	16.479	16.7553	1.555	−1.677
0.8	4.387	4.3187	16.098	16.3680	1.557	−1.677
1.0	4.364	4.2958	16.000	16.2687	1.563	−1.679

Table 4. Comparison of Nusselt number and friction factor data for a stationary rectangular duct for various aspect ratios

	Nu		*f Re*		% error	
AR	Exact	Present	Exact	Present	*Nu*	*f Re*
0.1	6.745	6.78495	21.4880	21.1688	0.5888	−1.5075
0.2	5.681	5.73769	19.3862	19.0705	0.9775	−1.6554
0.4	4.433	4.47185	16.5756	16.3681	0.8687	−1.2677
0.6	3.860	3.89456	15.1121	14.9799	0.8771	−0.8821
0.8	3.660	3.66382	14.4998	14.3778	0.0988	−0.8495
1.0	3.590	3.60795	14.3370	14.2271	0.4975	−0.7726

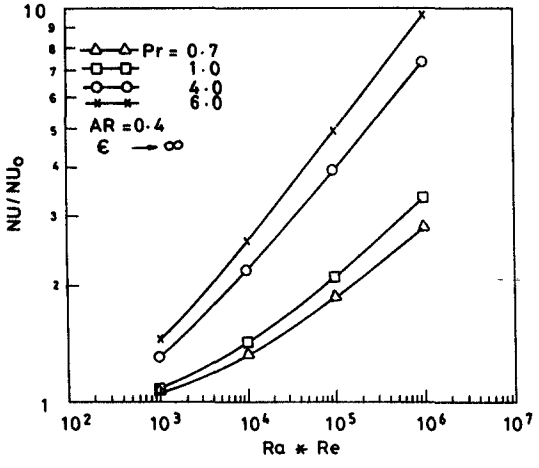

Fig. 5. Variation of heat transfer with rotation of an elliptical duct for various Prandtl numbers.

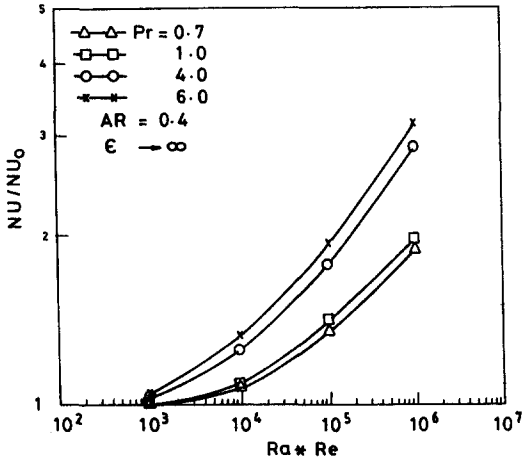

Fig. 6. Variation of heat transfer with rotation of a rectangular duct for various Prandtl numbers.

the enhancement of heat transfer by rotation, of the order of 3 to 4 times, when *Ra Re* is greater than 10^6. This enhancement is attributed to the effect of secondary flows consequent to rotation. From comparisons made on similar lines between the elliptical and rectangular ducts, it is noted that the relative enhancement of heat transfer due to rotation is more in the elliptical duct than in a comparable rectangular duct. This lower heat transfer efficiency of the rectangular duct is ascribed to the conditions inherent to the rectangular geometry, namely the sharp corners and the diminishing effect of corners on heat transfer.

The variation of the *f Re* ratio for rotating and stationary elliptical ducts for different Prandtl numbers is shown plotted in Fig. 7, against the parameter *Ra Re*, for an aspect ratio of 0.4. In Fig. 8, a similar plot is shown in the case of rectangular ducts. It is interesting to note that the effect on the friction factor is opposite to that on heat transfer as the Prandtl number is varied. It could be inferred that rotation is certainly more effective as better heat transfer is achieved for the same pumping power required for the stationary duct.

However, comparison between the results for elliptical ducts and rectangular ducts leads to the following observations. The relative increase in the pumping power between rotating and stationary ducts is more

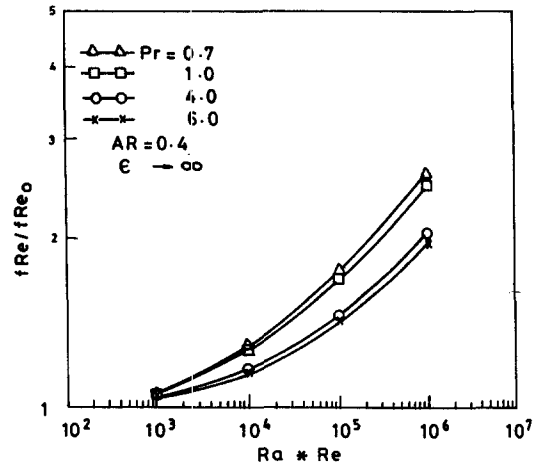

Fig. 7. Variation of pressure drop with rotation of an elliptical duct for various Prandtl numbers.

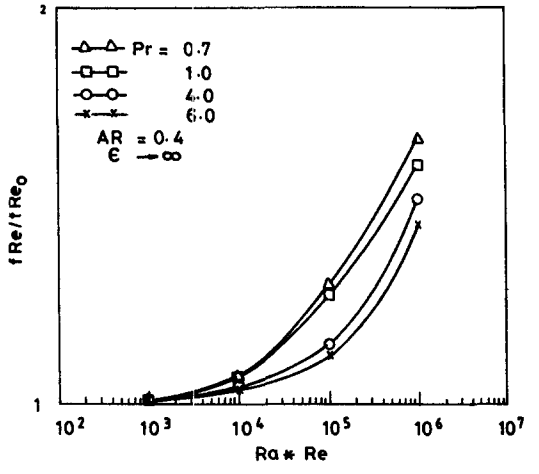

Fig. 8. Variation of pressure drop with rotation of a rectangular duct for various Prandtl numbers.

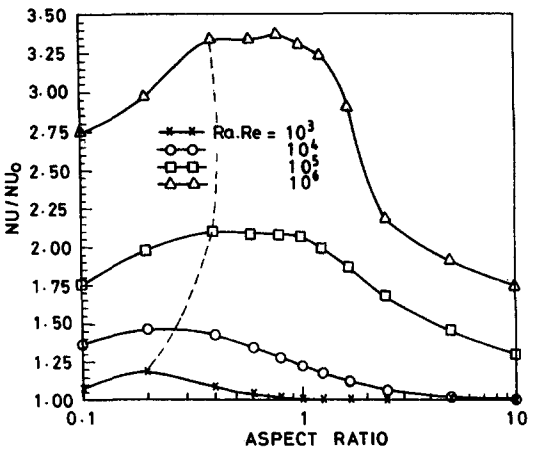

Fig. 9. Variation of Nusselt number with aspect ratio for various *Ra Re*, for an elliptical duct ($Pr = 1, \varepsilon \to \infty$).

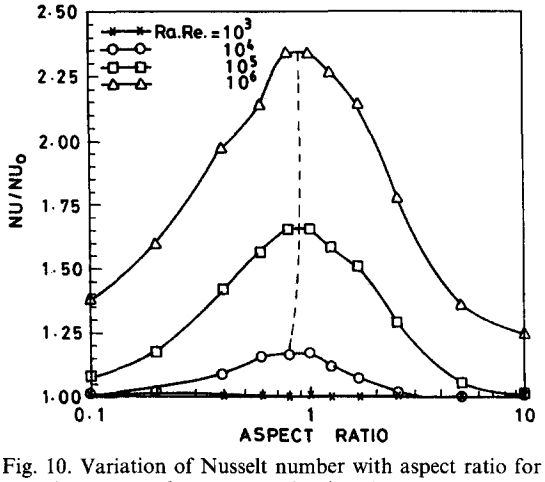

Fig. 10. Variation of Nusselt number with aspect ratio for various *Ra Re*, for a rectangular duct ($Pr = 1, \varepsilon \to \infty$).

in the elliptical ducts than in the rectangular ducts. But this has to be viewed in conjunction with the aforesaid fact that the relative enhancement in the heat transfer efficiency between the rotating and stationary ducts is higher in the case of elliptical ducts than it is for the rectangular ducts.

The variation of Nu/Nu_0 with aspect ratio for different values of *Ra Re* is shown in Fig. 9 for elliptical ducts. Each value of *Ra Re* represents a corresponding rotational speed. The bell-type course of the curves can be seen in the figure, suggesting a peak value for Nu/Nu_0 at a certain intermediate value of the aspect ratio. Also it is observed that with decreasing *Ra Re* the peak shifts towards lower aspect ratios. For any particular aspect ratio, the ratio Nu/Nu_0 increases with (*Ra Re*). Similar plots are shown in Fig. 10 for rectangular ducts. Comparison of the two figures establishes that the relative heat transfer enhancement due to rotation is higher in elliptical ducts than in rectangular ducts.

In Fig. 9, for elliptical ducts, the aspect ratio equal to unity actually corresponds to a circular duct, whereas the rest of the aspect ratios are related to elliptical ducts. As mentioned in the previous paragraph, for various values of decreasing *Ra Re* the peak value of Nu/Nu_0 shifts towards lower aspect ratios. This clearly indicates that, for decreasing speeds of rotation, the heat transfer efficiency of elliptical ducts is more than that of circular ducts. This observation can be conveniently exploited in optimizing the duct geometry for variable speed motors, especially in the speed range of 0–1000 rpm which lies within the range of *Ra Re* considered.

The variation of $fRe/(fRe)_0$ with aspect ratio for different values of *Ra Re* is shown in Figs. 11 and 12 respectively for elliptical and rectangular ducts. The trends are similar to the curves for Nu/Nu_0. One interesting observation, from a comparative evaluation of all the above four figures, is that for any particular aspect ratio, the ratio Nu/Nu_0 is greater than $fRe/(fRe)_0$, leading to the conclusion that the relative gain in heat transfer efficiency is more than the corresponding increase in the pumping power.

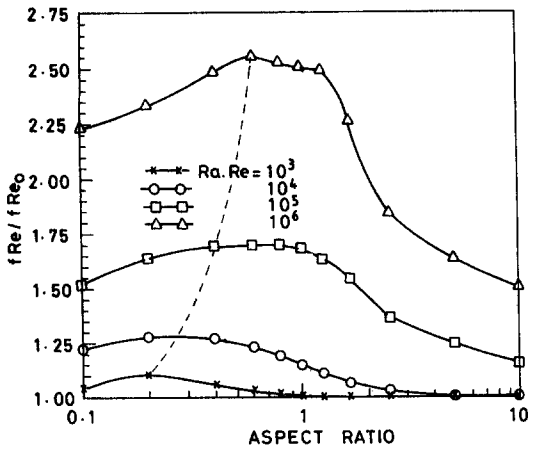

Fig. 11. Variation of friction factor with aspect ratio for various *Ra Re*, for an elliptical duct ($Pr = 1, \varepsilon \to \infty$).

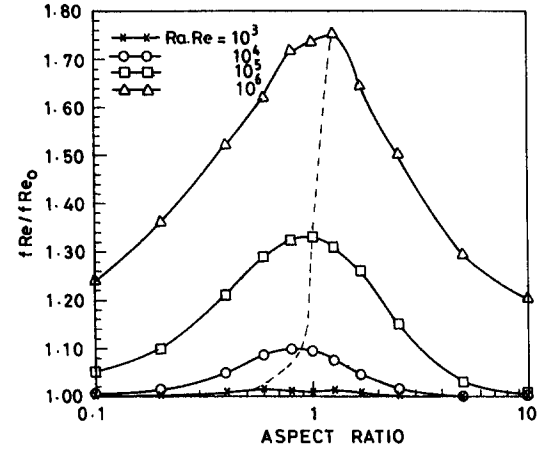

Fig. 12. Variation of friction factor with aspect ratio for various *Ra Re* for a rectangular duct ($Pr = 1, \varepsilon \to \infty$).

Figure 13 shows the variation of *Nu* with aspect ratio for stationary and rotating elliptical ducts and also for rectangular ducts. It may be seen that rotation enhanced the heat transfer in both cases. Similar plots are given in Fig. 14 for pressure drop. However, it may be recalled, as mentioned earlier, that the rise in heat transfer off-sets the rise in pumping power in the case of elliptical ducts.

Figures 15 and 16 respectively show the variation of heat transfer and pressure drop with eccentricity, in respect of both the elliptical and rectangular ducts. It can be seen that the effect of eccentricity is practically negligible beyond a value of 5.

It has been found that the effect of the rotational Reynolds number, *J*, is practically negligible within the range considered in the present study. This is in agreement with the earlier conclusions in the literature [3]. This is the reason why the ε and *J* are not included in the correlations to be presented.

In the graphs, wherever eccentricity, ε, and rotational Reynolds number, *J*, are expressed tending

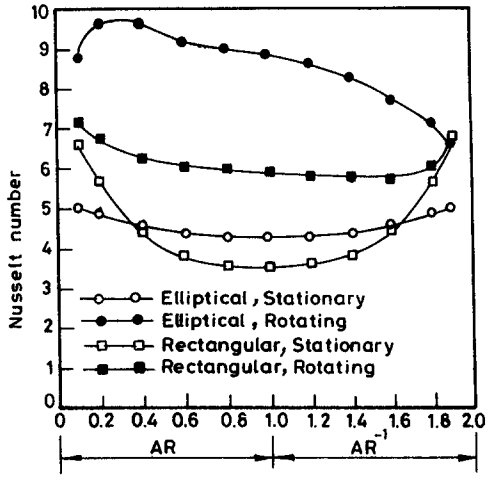

Fig. 13. Variation of Nusselt number with aspect ratio for stationary and rotating elliptical and rectangular ducts (*Ra Re* = 10^5, $Pr = 1, \varepsilon = \infty$).

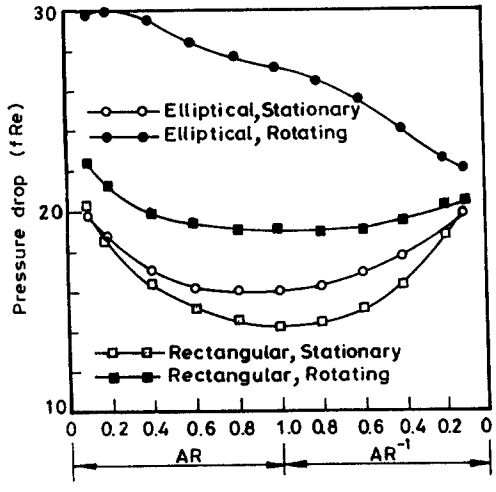

Fig. 14. Variation of pressure drop with aspect ratio for stationary and rotating elliptical and rectangular ducts (*Ra Re* = 10^5, $Pr = 1, \varepsilon = \infty$).

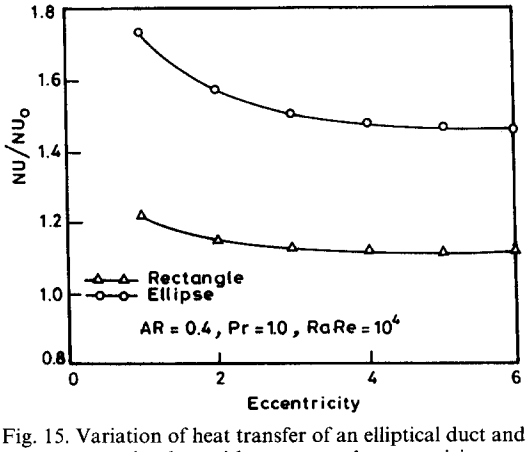

Fig. 15. Variation of heat transfer of an elliptical duct and a rectangular duct with respect to the eccentricity.

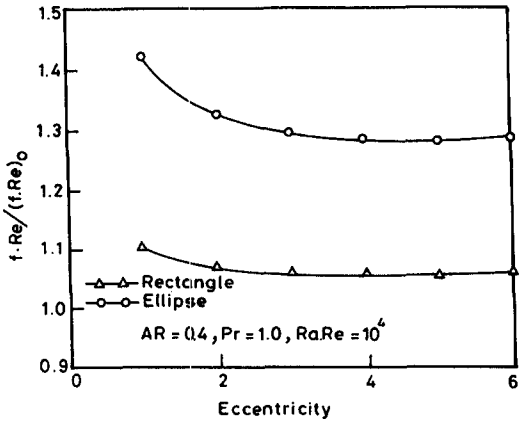

Fig. 16. Variation of pressure drop of an elliptical duct and a rectangular duct with respect to the eccentricity.

to infinity, the calculations were performed for very high values of these variables (i.e. $\varepsilon = 50$ and $J = 100$).

5.4. *Computational time*

The computational time needed for the solution of the equations in Table 1 was in general 1 second per 10 iterations on the SIEMENS-7580E system (5 MIPS). The number of iterations required for the solution of stationary ducts was around 40 with an over-relaxation factor of 1.75. For rotating ducts, the number of iterations was a very strong function of the product *Ra Re* and Prandtl number, *Pr*. Cases with rotation needed under-relaxation and the relaxation factor was varied between 0.5 and 0.7 depending on the parameters. A typical case with a combination of small values of *Pr* and *Ra Re* needed 400 iterations and one with large values required 1000 iterations. Convergence of the solution was treated as being achieved when the maximum residual error (fraction of the difference of the dependent variable between two consecutive iterations) was less than $\pm 0.5 \times 10^{-4}$.

5.5. *Correlations*

Heat transfer correlations for rectangular and elliptical duct, including the aspect ratio as an additional parameter are presented below.

Elliptical duct:

$$\frac{Nu}{Nu_0} = 0.27 AR^{-0.108} (Ra\,Re\,Pr)^{0.175}$$

(standard error is 0.09 and correlation coefficient is 0.922). Rectangular duct:

$$\frac{Nu}{Nu_0} = 0.5\left(AR + \frac{1}{AR}\right)^{-0.25} (Ra\,Re\,Pr)^{0.12}$$

(standard error is 0.048 and correlation coefficient is 0.937).

The range of the data used to obtain the above correlations has been already given in Table 2.

In the case of an elliptical duct, aspect ratio is taken as it is but for a rectangular duct $(AR + 1/AR)$ is taken as one parameter. This is because the Nu/Nu_0 variation in the case of a rectangular duct is almost symmetric about AR equal to one. This is not so for an elliptical duct. In fact, for a rectangular duct, an aspect-ratio range of $0 \leqslant AR \leqslant 1$ would have been sufficient. The above correlations, as special cases of an aspect ratio of unity should give results for a circular duct and rectangular duct. The correlation for a circular duct given in Morris [3] agrees well with the above correlation for AR equal to unity. However, there is a discrepancy in the case of a square duct.

6. CONCLUSIONS

The following main conclusions are drawn from the study:

- The numerical study reassures us that rotation enhances heat transfer.
- In comparison with stationary ducts, heat transfer and pressure drop increase with Prandtl number as well as (*Ra Re*) for both elliptical and rectangular rotating ducts for different aspect-ratios.
- The study established that, for aspect ratios less than 1, the relative rise in heat transfer compared with the relative rise in pumping power (the rise relative to the corresponding value under stationary conditions), is more in the case of rotating elliptical ducts. Hence the rotating elliptical ducts are considered to be more advantageous. However, this conclusion may not be true if the *Ra Re* product is outside the range considered. It should also be noticed that the manufacturing cost for an elliptical duct will be much more than for a circular one.

REFERENCES

1. R. K. Shah and A. L. London, Laminar flow forced convection in ducts. In *Advances in Heat Transfer*. Academic Press, New York (1978).
2. S. Kakac, R. K. Shah and W. Aung, *Handbook of Single Phase Convective Heat Transfer*. Wiley Interscience, New York (1987).
3. W. D. Morris, *Heat Transfer and Fluid Flow in Rotating Coolant Channels*. Research Studies Press, Wiley, New York (1981).
4. J. L. Woods and W. D. Morris, A study of heat transfer in a rotating cylindrical tube, *Trans ASME, J. Heat Transfer* **102**, 612–616 (1980).
5. A. K. Majumdar, W. D. Morris, D. Skiadaressis and D. B. Spalding, Heat transfer in rotating ducts, *Mech. Engng Bull.* **8**, 87–95 (1977).
6. W. D. Morris and F. M. Dias, Turbulent heat transfer in developing square sectioned tube, *J. Mech. Engng Sci.* **22**, (2) (1980).
7. N. Sarunac, S. Neti and E. K. Levy, Developing turbulent flow and heat transfer in axially rotating rectangular ducts, *ASME Winter Annual Meeting*, Anaheim, CA (1986).
8. S. Neti, A. S. Warnock, E. K. Levy and K. S. Kannan, Computation of laminar heat transfer in rotating rectangular ducts, *Trans ASME, J. Heat Transfer* **107**, 575–582 (1985).
9. A. D. Gosman *et al.*, *Heat and Mass Transfer in Recirculating Flows*. Academic Press, London and New York.
10. M. Mahadevappa, Numerical and experimental studies of fluid flow and heat transfer in rotating rectangular and elliptical ducts, Ph.D. Thesis, IIT Madras (1991).
11. E. Levy, S. Net, G. Brown, F. Bayat and V. Kadambi, Laminar heat transfer and pressure drop in a rectangular duct rotating about a parellal axis, *ASME J. Heat Transfer* **108**, 350–356 (1986).